Mineralogical Magazine (2019), **83**, 373–380
doi:10.1180/mgm.2018.122

CAMBRIDGE
UNIVERSITY PRESS

Article

Rinkite-(Y), $Na_2Ca_4YTi(Si_2O_7)_2OF_3$, a seidozerite-supergroup TS-block mineral from the Darai-Pioz alkaline massif, Tien-Shan mountains, Tajikistan: Description and crystal structure

Leonid A. Pautov[1], Atali A. Agakhanov[1], Vladimir Yu. Karpenko[1], Yulia A. Uvarova[2], Elena Sokolova[3]* and Frank C. Hawthorne[3]

[1]A.E. Fersman Mineralogical Museum, Russian Academy of Sciences, Leninskyi Prospekt 18-2, 119071 Moscow, Russia; [2]CSIRO Mineral Resources, ARRC, 26 Dick Perry Avenue, Kensington WA 6151 Australia; and [3]Department of Geological Sciences, University of Manitoba, 125 Dysart Road, Winnipeg, MB, R3T 2N2 Canada;

Abstract

Rinkite-(Y), ideally $Na_2Ca_4YTi(Si_2O_7)_2OF_3$, is a new rinkite-group (seidozerite-supergroup) TS-block mineral from the Darai-Pioz alkaline massif, Tian-Shan mountains, Tajikistan. The mineral is of hydrothermal origin. It occurs as aggregates (up to 1.5 cm long) of acicular crystals 0.1–1.0 mm thick, and as separate elongated columnar, flattened-prismatic crystals up to 1 cm long with rectangular or rhombic sections up to 0.5 mm across. Associated minerals are quartz, aegirine, microcline, neptunite, pectolite, calcite, eudialyte-group minerals, fluorite, titanite, turkestanite, kupletskite, galena, albite and pyrochlore-group minerals. Crystals are transparent and colourless to occasionally white, with a vitreous lustre. Rinkite-(Y) has a white streak, uneven, conchoidal fracture and does not fluoresce under a cathode or ultraviolet light. Cleavage is very good on {100}, no parting was observed, Mohs hardness is ~5, and it is brittle, $D_{\text{meas.}} = 3.44(2)$ g/cm^3, $D_{\text{calc.}} = 3.475$ g/cm^3. It is biaxial (+) with refractive indices ($\lambda = 590$ nm) $\alpha = 1.662(2)$, $\beta = 1.666(2)$, $\gamma = 1.685(5)$; $2V_{\text{meas.}} = 50(3)$ and $2V_{\text{calc.}} = 49.7°$. It is nonpleochroic. Rinkite-(Y) is monoclinic, space group $P2_1/c$, $a = 7.3934(5)$, $b = 5.6347(4)$, $c = 18.713(1)$ Å, $\beta = 101.415(2)°$ and $V = 764.2(2)$ Å^3. The six strongest reflections in the X-ray powder diffraction data [d(Å), I, (hkl)] are: 3.057, 100, (006, $\bar{2}12$, 210); 2.688, 28, (016); 9.18, 24, (002); 2.929, 17, ($\bar{2}13$, 211); 3.559, 15, (104, 014) and 2.783, 14, (021). The empirical formula calculated on 18 (O + F) is $Na_{2.11}(Ca_{3.74}Sr_{0.03}Mn_{0.03})_{\Sigma 3.80}(Y_{0.50}Nd_{0.16}Ce_{0.16}Gd_{0.07}Dy_{0.06}Sm_{0.05}Pr_{0.03}La_{0.03}U^{4+}_{0.01})_{\Sigma 1.07}(Ti_{0.85}Nb_{0.17}W^{6+}_{0.01}Ta_{0.01})_{\Sigma 1.04}(Si_{4.03}O_{14})O_{1.40}F_{2.60}$ with $Z = 2$. The ideal formula is $Na_2Ca_4YTi(Si_2O_7)_2OF_3$. The crystal structure was refined on a twinned crystal to $R_1 = 4.59\%$ on the basis of 1489 unique reflections ($F > 4\sigma F$) and is a framework of TS (Titanium-Silicate) blocks. The TS block consists of HOH sheets (H – heteropolyhedral, O – octahedral) parallel to (100). In the O sheet, the Ti-dominant $^{[6]}M^{O}1$ site ideally gives 1 Ti apfu. The $^{[8]}M^{O}2$ and $^{[6]}M^{O}3$ sites are ideally occupied by Na and (NaCa) apfu. In the H sheet, the $^{[7]}M^{H}$ site is occupied by $Ca_{1.13}Y_{0.50}REE_{0.37}$, ($REE$ = rare-earth element), ideally (CaY), $<M^{H}–\varphi> = 2.415$ Å and the $^{[7]}A^{P}$ site is occupied by $Ca_{1.81}REE_{0.19}$, ideally Ca_2, $<A^{P}–\varphi> = 2.458$ Å. The $M^{H} + A^{P}$ sites ideally give (Ca_3Y) apfu. The M^{H} and A^{P} polyhedra and Si_2O_7 groups constitute the H sheet. Linkage of H and O sheets via common vertices of M^{H} and A^{P} polyhedra and Si_2O_7 groups with $M^{O}1–3$ polyhedra results in a TS block. The TS block in rinkite-(Y) exhibits *linkage 1* and stereochemistry typical for the rinkite group (Ti = 1 apfu) of the seidozerite supergroup. For rinkite-(Y), the ideal structural formula of the form $A^{P}_{2}M^{H}_{2}M^{O}_{4}(Si_2O_7)_2(X^{O}_{M})_2(X^{O}_{A})_2$ is $(Ca_3Y)Na(NaCa)Ti(Si_2O_7)_2(OF)F_2$ with $Z = 2$. The mineral is named rinkite-(Y) as it is structurally identical to rinkite-(Ce) and Y is the dominant rare-earth element.

Keywords: rinkite-(Y), crystal-structure refinement, electron microprobe analysis, TS-block minerals, rinkite group, seidozerite supergroup, the Darai-Pioz alkaline massif, Tajikistan

(Received 22 January 2018; accepted 2 April 2018; Accepted Manuscript online: 29 June 2018; Associate Editor: Ian Graham)

Introduction

Rinkite-(Y) is a new mineral of the rinkite group in the seidozerite supergroup (Sokolova and Cámara, 2017). It is an Y-analogue of rinkite-(Ce), ideally $Na_2Ca_4REETi(Si_2O_7)_2OF_3$, where Ce is the dominant rare-earth element (Table 1). Rinkite-(Y) is also isostructural with nacareniobsite-(Ce) and mosandrite-(Ce) (Table 1). On formation of the seidozerite supergroup of TS-block minerals, Sokolova and Cámara (2017) changed the name rinkite to rinkite-(Ce). Hence, elsewhere in the paper we will refer to rinkite-(Ce) instead of just rinkite. The new mineral and its name have been approved by the Commission on New Minerals, Nomenclature and Classification, International Mineralogical Association (IMA2017-043, Pautov *et al.* 2017).

***Author for correspondence:** Elena Sokolova, Email: elena.sokolova@umanitoba.ca

Cite this article: Pautov L.A., Agakhanov A.A., Karpenko V.Y.u., Uvarova Y.A., Sokolova E., Hawthorne F.C. (2019) Rinkite-(Y), $Na_2Ca_4YTi(Si_2O_7)_2OF_3$, a seidozerite-supergroup TS-block mineral from the Darai-Pioz alkaline massif, Tien-Shan mountains, Tajikistan: Description and crystal structure. *Mineralogical Magazine* **83**, 373–380. https://doi.org/10.1180/mgm.2018.122

Table 1. The rinkite group of the seidozerite supergroup of TS-block minerals*, Ti (+ Nb + Zr) = 1 apfu.

Mineral Formula	Structure type	Ideal structural formula							Space group	Z	Ref.
		A_2^P	M_2^H	M_4^O		$(Si_2O_7)_2$	$(X_M^O)_2$	$(X_A^O)_2$			
Rinkite-(Ce) $Na_2Ca_4\mathit{REE}Ti(Si_2O_7)_2OF_3$	B1(GI)	Ca_2 $\Sigma\ A_2^P + M_2^H =$	$(Ca\mathit{REE})$ $(Ca_3\mathit{REE})$	Na(NaCa)	Ti	$(Si_2O_7)_2$	(OF)	F_2	$P2_1/c$	2	(1,2)
Rinkite-(Y) $Na_2Ca_4YTi(Si_2O_7)_2OF_3$	B1(GI)	Ca_2 $\Sigma\ A_2^P + M_2^H =$	(CaY) (Ca_3Y)	Na(NaCa)	Ti	$(Si_2O_7)_2$	(OF)	F_2	$P2_1/c$	2	(3)
Nacareniobsite-(Ce) $Na_3Ca_3\mathit{REE}Nb(Si_2O_7)_2OF_3$	B1(GI)	$(Ca,\mathit{REE})_2$ $\Sigma\ A_2^P + M_2^H =$	$(Ca,\mathit{REE})_2$ $(Ca_3\mathit{REE})$	Na_3	Nb	$(Si_2O_7)_2$	(OF)	F_2	$P2_1/c$	2	(4,5)
Mosandrite-(Ce) $[(H_2O)_2Ca_{0.5}\square_{0.5}]Ca_3\mathit{REE}Ti$ $(Si_2O_7)_2(OH)_2(H_2O)_2$	B1(GI)	Ca_2 $\Sigma\ A_2^P + M_2^H =$	$(Ca\mathit{REE})$ $(Ca_3\mathit{REE})$	$[(H_2O)_2$ $Ca_{0.5}\square_{0.5}]$	Ti	$(Si_2O_7)_2$	$(OH)_2$	$(H_2O)_2$	$P2_1/c$	2	(6,7)
Seidozerite $Na_4MnZr_2Ti(Si_2O_7)_2O_2F_2$	B2(GI)	Na_2 $\Sigma\ A_2^P + M_2^H =$	Zr_2 Na_2Zr_2	Na_2Mn	Ti	$(Si_2O_7)_2$	O_2	F_2	$P2/c$	2	(8,9)
Grenmarite $Na_4MnZr_3(Si_2O_7)_2O_2F_2$	B2(GI)	Na_2 $\Sigma\ A_2^P + M_2^H =$	Zr_2 Na_2Zr_2	Na_2Mn	Zr	$(Si_2O_7)_2$	O_2	F_2	$P2/c$	2	(10)
Götzenite $NaCa_6Ti(Si_2O_7)_2OF_3$	B3(GI)	Ca_2 $\Sigma\ A_2^P + M_2^H =$	Ca_2 Ca_4	$NaCa_2$	Ti	$(Si_2O_7)_2$	(OF)	F_2	$P\bar{1}$	1	(11,9)
Hainite-(Y) $Na_2Ca_4YTi(Si_2O_7)_2OF_3$	B3(GI)	Ca_2 $\Sigma\ A_2^P + M_2^H =$	(CaY) (Ca_3Y)	Na(NaCa)	Ti	$(Si_2O_7)_2$	(OF)	F_2	$P\bar{1}$	1	(12,13)
Fogoite-(Y) $Na_3Ca_2Y_2Ti(Si_2O_7)_2OF_3$	B3(GI)	Ca_2 $\Sigma\ A_2^P + M_2^H =$	Y_2 Ca_2Y_2	Na_3	Ti	$(Si_2O_7)_2$	(OF)	F_2	$P\bar{1}$	1	(14)
Batievaite-(Y) $Ca_2Y_2Ti(Si_2O_7)_2(OH)_2(H_2O)_4$	B3(GI)	Ca_2 $\Sigma\ A_2^P + M_2^H =$	Y_2 Ca_2Y_2	$[(H_2O)_2\square]$	Ti	$(Si_2O_7)_2$	$(OH)_2$	$(H_2O)_2$	$P\bar{1}$	1	(15)
Kochite $Na_3Ca_2MnZrTi(Si_2O_7)_2OF_3$	B3(GI)	Ca_2 $\Sigma\ A_2^P + M_2^H =$	Mn Zr Ca_2MnZr	Na_3	Ti	$(Si_2O_7)_2$	(OF)	F_2	$P\bar{1}$	2	(16)
Rosenbuschite $Na_6Ca_6Zr_3Ti(Si_2O_7)_4O_2F_6$	B3(GI)	Ca_4 $\Sigma\ A_4^P + M_4^H =$	$Ca_2\ Zr_2$ Ca_6Zr_2	Na_6	Ti Zr	$(Si_2O_7)_4$	$(OF)_2$	F_4	$P\bar{1}$	1	(17,9)

*Structure types, B (basic), and structural formula are from Sokolova and Cámara (2013) and Sokolova and Cámara (2017), respectively; formulae are per $(Si_2O_7)_2$, except per $(Si_2O_7)_4$ for rosenbuschite.

M^O and M^H = cations of the O and H sheets, A^P = cations at the peripheral (P) sites, X_4^O = anions of the O sheet not bonded to Si: X_M^O = anions at the common vertices of $3M^O$ and M^H polyhedra; X_A^O = anions at the common vertices of $3M^O$ and A^P polyhedra; atoms labelling is in accord with Sokolova (2006); composition of the M^O1 site is shown in red.

References (discovery of a mineral, the most recent structure work): (1) Lorenzen (1884); (2) Sample 1991C, Cámara *et al.* (2011); (3) this work; (4) Petersen *et al.* (1989); (5) Sokolova and Hawthorne (2008); (6) Brögger (1890); (7) Sokolova and Hawthorne (2013); (8) Semenov *et al.* (1958); (9) Christiansen *et al.* (2003*a*); (10) Bellezza *et al.* (2004); (11) Sahama and Hytönen (1957); (12) Blumrich (1893); (13) Lyalina *et al.* (2015); (14) Cámara *et al.* (2017); (15) Lyalina *et al.* (2016); (16) Christiansen *et al.* (2003*b*); and (17) Brögger (1887).

The holotype material is deposited in the collection of the Fersman Mineralogical Museum, Moscow, Russia, catalogue number 5043/1. The current paper reports the description and refinement of the crystal structure of rinkite-(Y).

Review of the relevant literature

Rinkite-(Ce) was originally described by Lorenzen (1884). Slepnev (1957) considered the mineralogy and crystal chemistry of rinkite-(Ce) and related minerals. Semenov (1963) and Mineev (1969) considered variations in the distribution of *REE* in some rinkite-group minerals and showed that Ce dominance is characteristic for minerals of this group. Semenov and Dusmatov (1975) described Y-rich rinkite-(Ce) (under the name "Y-rinkolite") from the Darai-Pioz massif. Based on chromatography analysis of "Y-rinkolite", they reported the following composition for the *REE* (wt.% from Σ*REE* = 100): La 9.2, Ce 33.0, Pr 6.9, Nd 23.6, Sm 3.5, Gd 5.0, Dy 2.50, Ho 0.70 and Y 15.6. Chakrabarty *et al.* (2013) reported a Nd-rich rinkite from the Sushina Hill Complex, India, with the following composition for the rare-earth elements (wt.% from Σ*REE* = 100): La 6.8, Ce 12.1, Pr 5.8, Nd 39.6, Sm 7.4, Gd 9.0, Dy 9.0 and Y 10.3. The first determination of the crystal structure of the type rinkite-(Ce) from Kangerdluarssuk, Greenland, was done by Kheirov *et al.* (1963) (space group $P\bar{1}$); then followed structure refinements in space group $P2_1$ by Tê-yü *et al.* (1965), Simonov and Belov (1968) and Rastsvetaeva *et al.* (1991). Galli and Alberti (1971) refined rinkite-(Ce) from Kangerdluarssuk, Greenland, in space group $P2_1/c$; the refinement of Sokolova and Cámara (2008) was in good agreement with the work of Galli and Alberti (1971). The most recent work on rinkite-(Ce) was done by Cámara *et al.* (2011). They refined the crystal structures of five rinkite-(Ce) crystals from three alkaline massifs (Ilímaussaq, Greenland; Khibiny, Kola Peninsula, Russia and Mt. St.-Hilaire, Canada) in space group $P2_1/c$ as two components related by the TWIN matrix ($\bar{1}$ 0 0/ 0 $\bar{1}$ 0/ 1 0 1); the crystals were analysed with an electron microprobe subsequent to collection of the X-ray data. Transmission electron microscopy confirmed the presence of pseudomerohedral twinning in sample 2909 of rinkite-(Ce) (Cámara *et al.*, 2011). Cámara *et al.* (2011) concluded that the lower symmetry described by the space group $P2_1$ was not justified for rinkite-(Ce). They said that the pseudomerohedral twins correspond to two different cell choices for space group No. 14. Pseudomerohedral twinning results in the apparent loss of the glide plane and apparent reduction of symmetry to space group $P2_1$. Rønsbo *et al.* (2014) reported on the rinkite-(Ce)-nacareniobsite-(Ce) solid-solution series from the Ilímaussaq alkaline complex.

Occurrence

Rinkite-(Y) occurs in the Darai-Pioz alkaline massif in the upper reaches of the Darai-Pioz River, Tajikistan [the Rasht (formerly Garm) district]. The area is near the junction of the Turkestansky, Zeravshansky and Alaisky ridges (39°30′N, 70° 40′E).

The multiphase Darai-Pioz massif belongs to the Upper Paleozoic Alaysky (Matchaisky) intrusive complex. The area of outcrop of the massif is ~16 km^2. Most of the massif rocks are covered by moraine or glaciers, and/or are difficult to access. In the north, the massif intrudes Silurian limestones and slates, and in the south, it intrudes terrigenous slates of Late Carboniferous age. The outer zone of the massif consists of sub-alkaline biotite granite, often tourmalinised (300–290 Ma), surrounding a discontinuous ring of biotite granites and granosyenites. The central part of the massif comprises quartz and aegirine syenites. In the northeast part of the massif, there is a stock of cancrinite and nepheline foyaite (247 ± 6 Ma). There are veins of syenite pegmatites and aegirine-potassium feldspar-quartz rocks containing polylithionite (286 ± 7 Ma) and various rare-metal and boron mineralisation. Veins of calcite carbonatites and syenite carbonatites (Faiziev *et al*., 2010) are widespread. Much of the rock is fenitised to various degrees. Detailed descriptions of the petrography and mineralogy of the Darai-Pioz massif can be found in Moskvin (1937), Dusmatov (1968, 1971), Semenov and Dusmatov (1975), Belakovskiy (1991) and Reguir *et al*. (1999).

Rinkite-(Y) has been found in a pegmatite fragment from the moraine of the Darai-Pioz glacier. The main minerals in this fragment are quartz, which forms a white medium-grained granulated aggregate, and microcline, which occurs as large white grains. Minor minerals are as follows: brownish-red eudialite, which forms crystals up to 3.5 cm in diameter, dark and henna-red neptunite which occurs as grains up to 1 cm in diameter, dark green columnar aegirine crystals up to 2 cm long, and accumulations of white calcite up to 2 cm in diameter. Accessory minerals are fluorite, galena, albite, pyrochlore-group minerals, pectolite, titanite, turkestanite, kupletskite and rinkite-(Y). So far, rinkite-(Y) has been found in only one sample.

Primary pegmatites with eudialyte and neptunite are exposed in the eastern wall of the glacial valley in the central part of the massif; they intrude quartz-bearing aegirine syenites. The veins are irregular, up to 1.5 m thick, and are commonly branched and weakly zoned. Contacts with the country rocks are weak, with a melanocrate aegirine zone. Toward the central part of a vein, there is a coarse-grained feldspar–aegirine zone, comprising microcline, albite, aegirine with minor titanite, eudialyte, neptunite, fluorite and pyrochlore-group minerals. The central part of the pegmatitic body is comprised of 80% white translucent quartz with calcite, eudialyte, fluorite, albite, titanite, neptunite and galena. It is highly probable that the pegmatite fragment with rinkite-(Y) comes from these veins.

Physical properties

Rinkite-(Y) occurs as aggregates up to 1.5 cm long, formed of acicular crystals 0.1–1.0 mm thick, and as separate elongated columnar flattened-prismatic crystals up to 1 cm long with rectangular or rhombic sections up to 0.5 mm across (Fig. 1*a*). Crystals are generally colourless to white (Fig. 1*b*), partly due to the presence of inclusions, and with a vitreous lustre. Rinkite-(Y) has a white streak, an uneven conchoidal fracture and does not fluoresce under a cathode or ultraviolet light. Cleavage is very good on {100} good, no parting was observed. The microhardness of rinkite-(Y) is $VHN_{100} = 569$ kg/mm^2 (547–659 range) which corresponds to a Mohs hardness of ~5; measurements were done on the PMT-3, calibrated on NaCl at a loading of 50 g. It is brittle, $D_{meas.} = 3.44(2)$ g/cm^3 (determined by flotation in Clerici liquid); $D_{calc.} = 3.475$ g/cm^3 (using the empirical formula and the single-crystal unit cell).

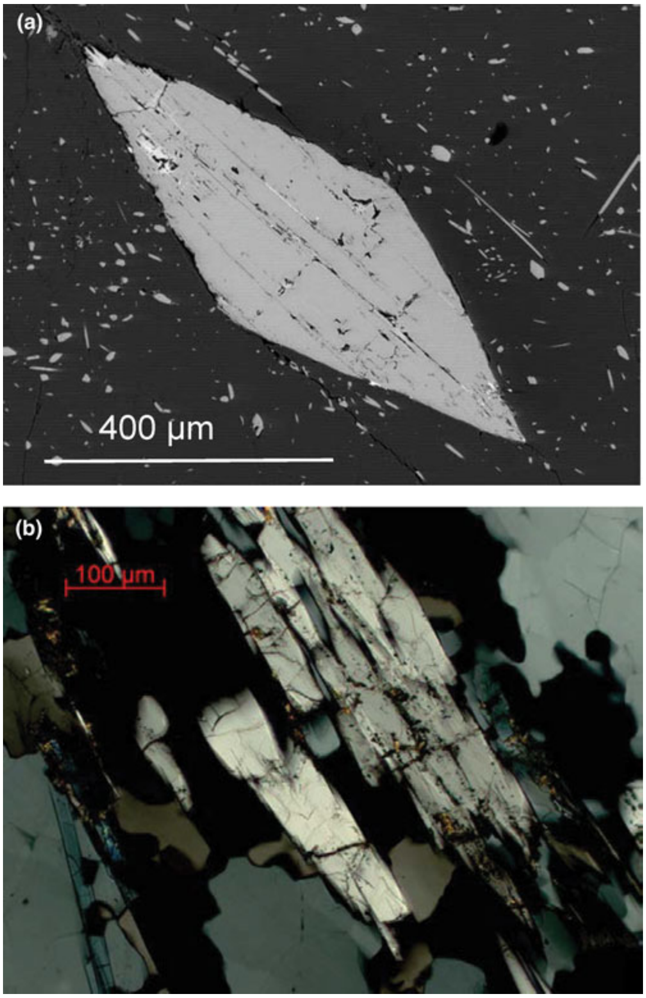

Fig. 1. Back-scattered electron image of a large crystal with typical rhombic section and numerous small crystals of rinkite-(Y) (pale-grey) in microcline (dark-grey) (*a*) and a photomicrograph under crossed-polars showing an intergrowth of rinkite-(Y) crystals (white) in a granular quartz aggregate (*b*).

Macroscopically, individual crystals do not show twinning. Rinkite-(Y) is biaxial (+) with refractive indices ($\lambda = 590$ nm) $\alpha = 1.662(2)$, $\beta = 1.666(2)$ and $\gamma = 1.685(5)$. The optic-axial plane occurs at an acute angle to the direction of elongation of the grains, and the maximum extinction angle relative to the elongation (Y) is 29°. The sign of elongation can be either positive, or negative, though for acicular grains, negative elongation is more common. The optic axial angle, measured with a Fyodorov stage, is 50(3)°, and $2V_{calc.} = 49.7°$. Rinkite-(Y) is non-pleochroic. Dispersion is medium: $v > r$. The compatibility index $(1 - K_p/K_c) = 0.035$ (for $D_{calc.} = 3.475$ g/cm^3) is rated as excellent (Mandarino, 1981).

Chemical analysis

A single crystal of rinkite-(Y) previously used for structure analysis was analysed using a Cameca SX-100 electron-microprobe operating in wavelength-dispersion mode with an accelerating voltage of 15 kV, a specimen current of 20 nA, a beam size of 2 µm and count times on peak and background of 20 and 10 s, respectively. The following standards were used: F: fluorite; Na:

Table 2. Chemical composition and unit formula for rinkite-(Y).

	wt.%	Range	Esd	Unit formula* (apfu)	
WO_3	0.41	0.29–0.47	0.06	Si	4.03
Ta_2O_5	0.15	0.05–0.25	0.06		
Nb_2O_5	2.74	2.56–2.88	0.09	Ti	0.85
UO_2	0.22	0.17–0.28	0.03	Nb	0.17
TiO_2	8.32	8.12–8.46	0.09	W^{6+}	0.01
SiO_2	29.51	29.26–29.87	0.20	Ta	0.01
Dy_2O_3	1.35	1.18–1.49	0.07	M^O1	1.04
Gd_2O_3	1.58	1.49–1.73	0.07		
Sm_2O_3	0.99	0.87–1.13	0.08	Na	2.11
Nd_2O_3	3.34	3.14–3.46	0.10	Ca	0.79
Pr_2O_3	0.61	0.52–0.70	0.05	Sr	0.03
Ce_2O_3	3.18	2.95–3.36	0.11	Mn	0.03
La_2O_3	0.56	0.47–0.74	0.07	$M^O(2,3)$	2.96
Y_2O_3	6.82	6.60–6.96	0.10		
SrO	0.35	0.22–0.44	0.07	Ca	2.95
MnO	0.28	0.25–0.33	0.02	Y	0.50
CaO	25.53	25.24–25.91	0.19	*REE***	0.56
Na_2O	7.98	7.85–8.15	0.09	U^{4+}	0.01
F	6.02	5.68–6.16	0.13	$M^H + A^P$	4.02
O = F	−2.53				
Total	97.41			Σcations	12.05
				O	15.40
				F	2.60
				Σanions	18.00

*Formula calculated on 18 (O + F)

***REE* = $(Nd_{0.16}Ce_{0.16}Gd_{0.07}Dy_{0.06}Sm_{0.05}Pr_{0.03}La_{0.03})_{\Sigma 0.56}$

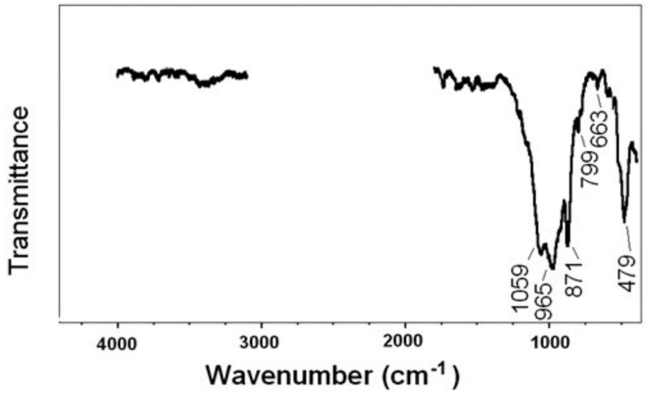

Fig. 2. The IR-spectrum of rinkite-(Y): the region from 400 to1800 cm^{-1} was recorded from a KBr pellet and the region from 400 to 1800 cm^{-1}, from finely-ground rinkite-(Y) dispersed in Nujol; the region from ~3000 to 1750 cm^{-1} is omitted as it contains the major peaks from Nujol in which the rinkite-(Y) was suspended.

albite; Si, Ca: diopside; Nb: $Ba_2NaNb_5O_{15}$; Mn: spessartine; Ce: $CePO_4$; La: $LaPO_4$; Nd: $NdPO_4$; Pr: $PrPO_4$; Sm: $SmPO_4$; Gd: $GdPO_4$; Dy: $DyPO_4$; Ti: titanite; Sr: $SrTiO_3$; Y: $Y_3Al_5O_{12}$ and Ta: $Mn(Ta_{1.7}Nb_{0.3})O_6$. The elements Zr, Ba, Th, Hf, K, Mg, Fe and Al were sought but not detected. Data were reduced using the φ(ρZ) procedure of Pouchou and Pichoir (1985). The chemical composition of rinkite-(Y) is the mean of 10 determinations and is given in Table 2. The empirical formula calculated on 18 (O + F) is $Na_{2.11}(Ca_{3.74}Sr_{0.03}Mn_{0.03})_{\Sigma 3.80}(Y_{0.50}Nd_{0.16}Ce_{0.16}Gd_{0.07}Dy_{0.06}Sm_{0.05}Pr_{0.03}La_{0.03}U^{4+}_{0.01})_{\Sigma 1.07}(Ti_{0.85}Nb_{0.17}W^{6+}_{0.01}Ta_{0.01})_{\Sigma 1.04}(Si_{4.03}O_{14})O_{1.40}F_{2.60}$ with $Z = 2$. For rinkite-(Y), the ideal structural formula of the form $A^P_2M^H_2M^O_4(Si_2O_7)_2(X^O_M)_2(X^O_A)_2$ is $(Ca_3Y)Na(NaCa)Ti(Si_2O_7)_2(OF)F_2$ with $Z = 2$. The ideal formula is $Na_2Ca_4YTi(Si_2O_7)_2OF_3$.

Table 3. X-ray powder-diffraction data for rinkite-(Y)

I_{obs}	I_{calc}	d_{obs}(Å)	d_{calc}(Å)	*h k l*	I_{obs}	I_{calc}	d_{obs}(Å)	d_{calc}(Å)	*h k l*
24	**25**	**9.18**	**9.172**	**0 0 2**	3	7	2.138	2.138	$\bar{2}$ 0 8
3	5	7.22	7.247	1 0 0		7		2.137	2 0 6
2	6	5.39	5.386	0 1 1	3	5	2.125	2.124	0 1 8
1	2	4.81	4.801	0 1 2	1	4	2.104	2.104	$\bar{2}$ 2 4
2	2	4.45	4.448	1 1 0		5		2.104	2 2 2
8	7	4.26	4.276	$\bar{1}$ 0 4	2	5	2.071	2.072	0 2 6
3	9	4.205	4.208	$\bar{1}$ 1 2	8	27	2.012	2.013	2 2 3
	4		4.208	1 1 1	2	2	1.917	1.919	0 2 7
4	10	4.149	4.144	0 1 3		4		1.913	$\bar{2}$ 2 6
3	10	3.827	3.825	$\bar{1}$ 1 3	8	53	1.842	1.848	$\bar{4}$ 0 2
	2		3.824	1 1 2		18		1.842	$\bar{2}$ 1 9
15	**10**	**3.559**	**3.569**	**1 0 4**		19		1.841	2 1 7
	36		3.557	0 1 4	4	20	1.807	1.808	$\bar{2}$ 2 7
100	**58**	**3.057**	**3.057**	**0 0 6**		19		1.807	2 2 5
	100		3.048	$\bar{2}$ 1 2	1	7	1.778	1.778	0 2 8
	92		3.048	2 1 0	2	5	1.743	1.744	0 1.10
5	3	3.006	3.015	1 1 4	1	1	1.728	1.725	4 1 0
17	**46**	**2.929**	**2.929**	**$\bar{2}$ 1 3**	2	4	1.701	1.702	$\bar{2}$ 1.10
	42		2.929	2 1 1		4		1.701	2 1 8
14	**52**	**2.783**	**2.785**	**0 2 1**	7	40	1.673	1.675	$\bar{2}$ 3 1
28	**61**	**2.688**	**2.687**	**0 1 6**		16		1.672	0 3 5
4	6	2.608	2.605	$\bar{2}$ 0 6	2	4	1.599	1.599	0 1.11
7	14	2.561	2.563	$\bar{2}$ 1 5	2	7	1.581	1.582	$\bar{4}$ 0 8
	14		2.563	2 1 3		7		1.582	4 0 4
3	14	2.399	2.401	0 2 4	2	9	1.522	1.523	$\bar{4}$ 1 8
4	11	2.377	2.376	0 1 7		9		1.523	4 1 4
1	2	2.326	2.322	$\bar{1}$ 0 8	3	6	1.475	1.475	0 1.12
15	15	2.293	2.293	0 0 8	2	9	1.522	1.523	$\bar{4}$ 1 8
5	11	2.175	2.177	$\bar{2}$ 2 3		9		1.523	4 1 4
	12		2.177	2 2 1	3	6	1.475	1.475	0 1.12
	2		2.174	$\bar{2}$ 1 7					

The strongest lines are given in bold.

Table 4. Miscellaneous refinement data for rinkite-(Y).

Crystal data	
Ideal formula	$Na_2Ca_4YTi(Si_2O_7)_2OF_3$
Crystal dimensions (mm)	0.20 × 0.16 × 0.08
Crystal system, space group	Monoclinic, $P2_1/c$
Temperature (K)	293(2)
a, *b*, *c* (Å)	7.3934(5), 5.6347(4), 18.713(1)
β(°)	101.415(2)
V ($Å^3$)	764.2(2)
Z	2
Absorption coefficient (mm^{-1})	6.49
F(000)	767.9
$D_{calc.}$ (g/cm^3)	3.475
Data collection	
Crystal description	Flattened prism
Radiation/monochromator	Mo*K*α/ graphite
$2\theta_{max}$ (°)	59.94*, 54.98**
R_{int} (%)	4.65**
Second component (%)***	55.8(3)
Reflections collected	6354**
Independent reflections	1802**
$F_o > 4\sigma F$	1489**
Refinement	
Refinement method	Full-matrix least squares on F^2, fixed weights proportional to $1/\sigma F_o^2$
Final R_{obs} (%)	
R_1 [$F_o > 4\sigma F$]	4.59
R_1 (all data), wR_2	5.77, 13.36
Goodness of fit on F^2	1.046
Number of refined parameters	146
$\Delta\rho_{max}$, $\Delta\rho_{min}$ ($e^- Å^{-3}$)	2.145, −1.193

* Data collection; **structure refinement; ***second component of the crystal is related to the first component by the twin matrix [$\bar{1}$ 0 0/ 0 $\bar{1}$ 0/ 1 0 1].

Table 5. Atom coordinates and anisotropic displacement parameters (Å^2) for rinkite-(Y).

Atom	*x*	*y*	*z*	U_{eq}	U^{11}	U^{22}	U^{33}	U^{23}	U^{13}	U^{12}
M^{H}	0.0951(2)	0.65858(12)	0.19318(3)	0.0101(2)	0.0049(5)	0.0105(4)	0.0150(4)	0.0012(3)	0.0019(9)	0.0001(7)
A^{P}	0.5972(3)	0.65996(17)	0.19072(4)	0.0132(3)	0.0086(7)	0.0139(5)	0.0172(5)	0.0004(4)	0.0028(12)	0.0006(10)
$M^{O}1$	0	0	0	0.0314(6)	0.0015(9)	0.0606(12)	0.0332(10)	−0.0353(9)	0.0060(16)	−0.0074(18)
$M^{O}2$	½	0	0	0.0237(12)	0.027(2)	0.025(2)	0.018(2)	−0.0053(14)	0.002(4)	−0.004(4)
$M^{O}3$	0.7511(2)	0.5010(4)	−0.00034(10)	0.0233(7)	0.0198(16)	0.0175(10)	0.0320(11)	0.0062(7)	0.004(3)	−0.003(3)
Si1	0.3484(3)	0.1527(4)	0.14031(9)	0.0121(5)	0.0116(14)	0.0112(8)	0.0135(8)	−0.0002(7)	0.0025(6)	−0.0002(15)
Si2	0.7855(2)	0.1518(4)	0.13764(9)	0.0101(5)	0.0063(13)	0.0114(8)	0.0130(8)	−0.0008(7)	0.0025(6)	0.0005(14)
O1	0.2150(6)	0.1497(11)	0.0614(2)	0.0180(10)	0.012(2)	0.018(2)	0.021(2)	0.003(2)	−0.0047(16)	−0.006(2)
O2	0.8341(6)	0.1425(11)	0.0578(2)	0.0176(10)	0.017(2)	0.020(2)	0.018(2)	0.000(2)	0.0076(16)	0.003(2)
O3	0.3335(12)	0.3938(8)	0.1851(2)	0.0136(10)	0.009(3)	0.011(2)	0.021(2)	−0.0056(16)	0.004(4)	0.007(4)
O4	0.8452(13)	0.3944(9)	0.1817(2)	0.0184(11)	0.012(2)	0.018(3)	0.023(2)	−0.0055(19)	−0.001(4)	0.014(4)
O5	0.3319(11)	0.9267(9)	0.1917(2)	0.0126(11)	0.010(3)	0.014(2)	0.013(2)	0.0011(15)	0.001(3)	−0.003(3)
O6	0.8507(13)	0.9268(8)	0.1901(2)	0.0137(10)	0.016(2)	0.009(2)	0.016(2)	0.0033(15)	0.002(4)	0.002(4)
O7	0.5575(6)	0.1443(10)	0.1210(2)	0.0248(10)	0.015(2)	0.038(3)	0.022(2)	−0.004(2)	0.008(2)	0.000(3)
X^{O}_{M}	0.0288(15)	0.7012(7)	0.0632(2)	0.0220(12)	0.016(2)	0.027(2)	0.022(2)	−0.0035(18)	0.003(3)	0.003(3)
X^{O}_{A}	0.5297(16)	0.6557(7)	0.0642(2)	0.0261(9)	0.032(2)	0.0264(19)	0.0185(18)	0.0030(16)	0.002(3)	0.001(4)

Table 6. Selected interatomic distances (Å) and angles (°) in rinkite-(Y).

M^{H}–O5	2.317(7)		A^{P}–X^{O}_{A}	2.322(4)			
M^{H}–O3	2.337(7)		A^{P}–O4	2.398(8)			
M^{H}–O6(a)	2.348(8)		A^{P}–O6	2.405(8)			
M^{H}–O4(a)	2.349(9)		A^{P}–O3	2.446(8)			
M^{H}–X^{O}_{M}	2.397(4)		A^{P}–O5	2.474(8)			
M^{H}–O6(b)	2.507(4)		A^{P}–O5(b)	2.528(5)			
M^{H}–O4(c)	2.652(5)		A^{P}–O3(c)	2.632(5)			
<$M^{H}1$–φ>	2.415		<A^{P}–φ>	2.458			
$M^{O}1$–O1	1.958(4)	×2	$M^{O}2$–X^{O}_{A}(f)	2.269(4)	×2	$M^{O}3$–O1(f)	2.314(6)
$M^{O}1$–O2(a)	1.960(4)	×2	$M^{O}2$–O7	2.363(5)	×2	$M^{O}3$–O2	2.319(6)
$M^{O}1$–X^{O}_{M}(d)	2.044(4)	×2	$M^{O}2$–O2	2.619(4)	×2	$M^{O}3$–X^{O}_{A}(f)	2.353(9)
<$M^{O}1$–φ>	1.987		$M^{O}2$–O1	2.726(5)	×2	$M^{O}3$–X^{O}_{A}	2.383(10)
			<$M^{O}2$–φ>	2.494		$M^{O}3$–X^{O}_{M}(g)	2.436(9)
						$M^{O}3$–X^{O}_{M}(f)	2.466(9)
						<$M^{O}3$–φ>	2.378
Si1–O1	1.605(4)		Si2–O2	1.606(4)			
Si1–O3	1.611(5)		Si2–O4	1.613(6)		Si1–O7–Si2	156.8(3)
Si1–O5(e)	1.615(5)		Si2–O6(e)	1.618(5)			
Si1–O7	1.657(5)		Si2–O7	1.653(5)			
<Si1–O>	1.622		<Si2–O>	1.623			

φ = O or F

Symmetry operators (given in brackets): a: *x*–1, *y*, *z*; b: –*x* + 1, *y*–½, –*z*+½; c: –*x* + 1, *y*+½, –*z*+½; d: –*x*–1, –*y* + 1, –*z*; e: *x*, *y*–1, *z*; f: –*x* + 1, –*y* + 1, –*z*; g: *x* + 1, *y*, *z*.

Infrared spectroscopy

The infrared (IR) spectrum in the range 400–1800 cm^{-1} was recorded from a KBr pellet and in the range 3000–4000 cm^{-1} from finely-ground rinkite-(Y) dispersed in Nujol with a Specord 75IR spectrometer (Carl Zeiss, Jena). The spectrum is shown in Fig. 2; the region from ∼3000–1800 cm^{-1} is omitted as it contains the major peaks from Nujol. The observed bands (cm^{-1}) are as follows: 1158, 1059, 965 and 871 (Si–O-stretching vibrations), 799, 775 and 663 (O–Si–O bending vibrations of Si_2O_7 groups), 587 and 561 (Ti–O-stretching vibrations) and 479 (Si–O–Si bending and stretching vibrations). There are no bands around 3500 and ∼1630 cm^{-1}, indicating the absence of H_2O and OH^- groups, in accord with the refined crystal structure.

Powder X-ray diffraction

Powder X-ray diffraction data for rinkite-(Y) were collected with a DRON-2.0 diffractometer with Fe*K*α radiation and are given in Table 3. Unit-cell parameters refined from the powder data are as follows: $a = 7.3934(5)$, $b = 5.6347(4)$, $c = 18.713(1)$ Å, β 101.415(2)° and $V = 762.2(2)$ Å^3.

X-ray data collection and structure refinement

X-ray single-crystal data for rinkite-(Y) were collected from a twinned crystal with a single-crystal Bruker P4 four-circle diffractometer equipped with a graphite monochromator (Mo*K*α radiation), multilayer optics and Smart 1K CCD detector. Details of data collection and structure refinement are given in Table 4. The intensities of reflections with $-8 \le h \le 10$, $-7 \le k \le 7$, $-26 \le l \le 26$ were collected with a frame width of 0.2° and a frame time of 30 s, and an empirical absorption correction (*SADABS*, Sheldrick, 2008) was applied. We observed 115 violations (> 3σ*F*) of the *c*-glide extinction criterion and refined the structure as two components related by the TWIN matrix ($\bar{1}$ 0 0/ 0 $\bar{1}$ 0/ 1 0 1) (see discussion on the nonmerohedral twinning in rinkite-(Ce) in Cámara *et al.*, 2011). There were few observed reflections at high 2θ, and those that do occur show splitting due to pseudomerohedral twinning, and refinement of the structure was carried out for $2\theta \le 55°$, $-8 \le h \le 9$, $-7 \le k \le 7$, $-24 \le l \le 24$. The crystal-structure refinement was undertaken with Bruker *SHELXTL Version 5.1* (Sheldrick, 2015) in space group $P2_1/c$ using the atom coordinates of rinkite-(Ce) (Cámara *et al.*, 2011). The crystal structure of rinkite-(Y) was refined to $R_1 = 4.59\%$, the twin ratio being 0.558(3):0.442(3) (Table 4). The occupancies of five cation sites were refined with the following scattering curves: M^{H} and A^{P} sites: Y; $M^{O}1$ site: Ti; $M^{O}2$ and $M^{O}3$ sites: Na and Ca, respectively (for the site-labelling see footnote of Table 1). The occupancies of the X^{O}_{M} and X^{O}_{A} anion sites were refined with the scattering curve of F; refinement of the X^{O}_{A} site occupancy converged to an integer value (within 3 e.s.d.) and was subsequently fixed at full occupancy. Scattering curves for neutral atoms were taken from the *International Tables for Crystallography* (Wilson, 1992). Final atom coordinates and equivalent displacement parameters are given in Table 5, selected interatomic distances and angles in Table 6, refined site-scattering values and assigned site-populations in Table 7, and bond-valence values for selected anions in Table 8. A list of observed and calculated structure factors and crystallographic information file have been deposited with the Principal Editor of *Mineralogical Magazine* and are available as Supplementary material (see below).

Table 7. Refined site scattering and assigned site-populations for rinkite-(Y)

Site*	Refined site scattering (epfu)	Assigned site population (apfu)	Calculated site scattering (epfu)	<Cation–φ>$_{obs.}$ (Å)	<Cation-φ>$_{calc.}$** (Å)	Ideal composition (apfu)
		Cations				
$^{[7]}M^{H}$	67.6(3)	$Ca_{1.13}Y_{0.50}REE_{0.37}$***	64.50	2.415	2.416	(CaY)
$^{[7]}A^{P}$	51.3(3)	$Ca_{1.81}REE_{0.19}$***	47.70	2.458	2.440	Ca_2
$M^{H}+A^{P}$	118.9	$Ca_{2.94}REE_{0.56}Y_{0.50}$	112.20			(Ca_3Y)
$M^{O}1$	24.0(2)	$Ti_{0.85}Nb_{0.15}$	24.85	1.987	1.990	Ti
$^{[8]}M^{O}2$	11.7(2)	$Na_{0.96}Sr_{0.03}\square_{\mathbf{0.01}}$	11.70	2.494	2.550	Na
$M^{O}3$	29.1(3)	$Na_{1.15}Ca_{0.79}Mn_{0.03}\square_{\mathbf{0.03}}$	29.20	2.378	2.373	(NaCa)
$\Sigma\ M^{O}(2,3)$	40.8	$Na_{2.11}Ca_{0.79}Sr_{0.03}Mn_{0.03}\square_{\mathbf{0.04}}$	40.90			Na(NaCa)
		Anions				
X^{O}_{M}	17.0(2)	$O_{1.40}F_{0.60}$	16.60			(OF)
X^{O}_{A}	18.00	F_2	18.00			F_2

*Coordination numbers are shown for non-[6]-coordinated cation sites; **distances < Cation–φ> were calculated using ionic radii of Shannon (1976), φ = O or F;
***$REE = (Nd_{0.16}Ce_{0.16}Gd_{0.07}Dy_{0.06}Sm_{0.05}Pr_{0.03}La_{0.03})_{\Sigma 0.56}$, with $f_{av} = 60.54$ *el*.

Table 8. Bond-valence values* for X^{O}_{M} and X^{O}_{A} anions in rinkite-(Y).

Cation	$X^{O}_{M}(O_{0.7}F_{0.3})$	$X^{O}_{A}(F)$
$M^{H}(Ca_{0.5}Y_{0.25}Ce_{0.25})$	0.38	
$A^{P}(Ca)$		0.29
$M^{O}1(Ti)$	0.49	
$M^{O}2(Na)$		0.19
$M^{O}3(Na_{0.5}Ca_{0.5})$	0.23	0.22
	0.22	0.20
Σ	1.32	0.90

*Bond-valence parameters (vu) are from Brown (1981).

Table 9. Comparison of rinkite-(Y) and rinkite-(Ce)*.

Mineral	Rinkite-(Y)	Rinkite-(Ce)
Ideal formula	$Na_2Ca_4YTi(Si_2O_7)_2OF_3$	$Na_2Ca_4REETi(Si_2O_7)_2OF_3$ *REE* = Ce
Space group	$P2_1/c$	$P2_1/c$
a (Å)	7.3934	7.4132–7.4414
b	5.6347	5.6595–5.7083
c	18.713	18.8181–18.9410
α (°)	90	90
β	101.415	101.353–101.424
γ	90	90
Z	2	2
$D_{calc.}$ (g cm^{-3})	3.475	3.363–3.502
$D_{meas.}$ (g cm^{-3})	3.44	3.18–3.44
Strongest reflections in the powder X-ray diffraction data, *d*/Å (*I*)	9.18(24)	9.236(7)
	3.559(15)	3.583(21)
	3.057(100)	3.061(100)
	2.929(17)	2.943(40)
	2.783(14)	2.807(30)
	2.688(28)	2.707(39)
Optical class, sign	biaxial (+)	biaxial (+)
α (590 nm)	1.663	1.643–1.662
β	1.667	1.645–1.667
γ	1.686	1.651–1.681
$2V_{meas.}$ (°)	50	43–87
$2V_{calc.}$ (°)	49.7	–

*Rinkite-(Ce): ideal formula, crystallographic data and $D_{calc.}$ for the six samples of rinkite-(Ce) are from Cámara *et al.* (2011) and Sokolova and Cámara (2008); $D_{meas.}$ and optical data are from Anthony *et al.* (1995), powder X-ray diffraction data, from JCPDS 71-0440 [powder diffraction file from the International Centre for Diffraction Data (http://www.icdd.com/)].

Site-population assignment

There are seven cation sites in the crystal structure of rinkite-(Y): three M^{O} sites of the O sheet and the M^{H}, A^{P} and two *Si* sites of the H sheet; site labelling is in accord with Sokolova (2006). Consider first the Ti-dominant $M^{O}1$ site. We assign cations to this site based on our previous work on rinkite-(Ce) (Cámara *et al.*, 2011): Ti-dominant sites are always fully occupied. We assign $Ti_{0.85}Nb_{0.15}$ apfu to the $M^{O}1$ site, with refined and calculated scattering values of 24.0 and 24.85 electrons per formula unit (epfu), respectively (Table 7). Such assignment is supported by matching values of observed and calculated mean bond lengths of 1.987 and 1.990 Å, respectively (Tables 6, 7).

Consider next the $^{[8]}M^{O}2$ and $^{[6]}M^{O}3$ sites in the O sheet occupied by alkali cations. In accord with structure-refinement results for rinkite-(Ce) (Cámara *et al.*, 2011), we assign $Na_{0.96}Sr_{0.03}\square_{0.01}$ to the $M^{O}2$ site and $Na_{1.15}Ca_{0.79}Mn_{0.03}\square_{0.03}$ to the $M^{O}3$ site. These assignments are supported by close agreement between (1) refined and calculated scattering values of 11.7 and 11.70 epfu for the $M^{O}2$ site and 29.1 and 29.20 epfu for the $M^{O}3$ site, and (2) observed and calculated mean bond lengths of 2.494 and 2.550 Å for the $M^{O}2$ site and 2.378 and 2.373 Å for the $M^{O}3$ site (Tables 6, 7).

Consider next the two [7]-coordinated M^{H} and A^{P} sites in the H sheet. In rinkite-(Ce), these sites are fully occupied mainly by Ca and REE^{3+} in the ratio ~3:1 (Cámara *et al.*, 2011). The cations to be assigned to the M^{H} and A^{P} sites are $Ca_{2.95}Y_{0.50}REE_{0.56}U^{4+}_{0.01}$, with a total calculated scattering of 113.32 epfu (Table 2). The $< M^{H}–φ>$ distance of 2.415 Å is shorter than the $<A^{P}–φ>$ distance of 2.458 Å (where φ = O or F) (Table 6) and hence we assign all (smaller) Y (radius = 0.96 Å, Shannon, 1976) to the M^{H} site (Table 7). The scattering at the A^{P} site is lower than that at the M^{H} site, and we distribute Ca and *REE* at the M^{H} and A^{P} sites so their calculated site-scattering values are in the same ratio as the corresponding refined values. The two latter assignments are supported by close agreement between the observed and calculated mean bond lengths of 2.415 and 2.416 Å for the M^{H} site and 2.458 and 2.440 Å for the A^{P} site (Table 7).

There are nine anion sites in the crystal structure of rinkite-(Y). We assign O atoms to the O(1–7) sites that constitute the tetrahedral coordination of the *Si*1 and *Si*2 sites. Anions at two sites, X^{O}_{M} and X^{O}_{A}, receive bond valence from four cations, [$M^{O}1$, $2M^{O}3$ and M^{H}] and [$M^{O}2$, $2M^{O}3$ and A^{P}], respectively (Table 8). We expect the X^{O}_{M} atom to receive a higher bond valence as it is bonded to Ti at the $M^{O}1$ site, and the X^{O}_{A} atom, a lower bond-valence as it is bonded to Na at the $M^{O}2$

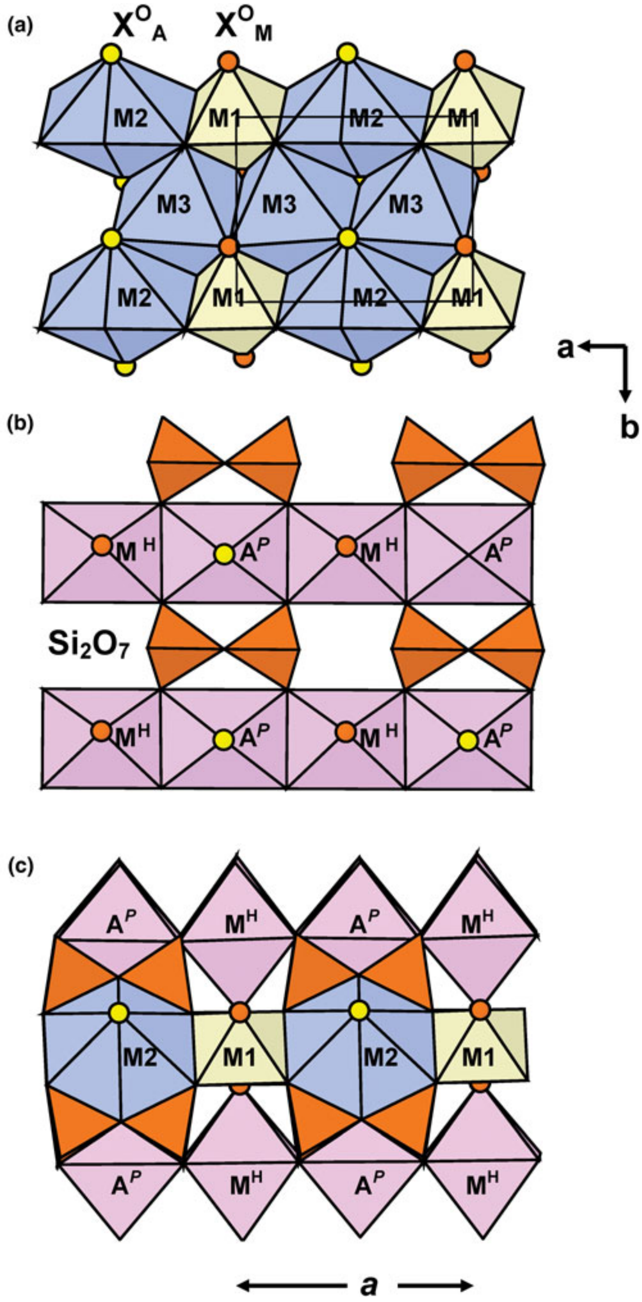

Fig. 3. The details of the TS (Titanium-Silicate) block in the structure of rinkite-(Y): the close-packed O sheet of [8]Na-polyhedra, (NaCa) octahedra and Ti octahedra (*a*); the H sheet of [7]-coordinated Ca-dominant polyhedra and Si_2O_7 groups (*b*); and linkage of O and H sheets in the TS block (*c*). SiO_4 tetrahedra are orange, Ti-dominant, Ca-dominant and Na + (NaCa) polyhedra are pale yellow, pink and navy blue, respectively; F (X^O_A site) and (OF) (X^O_M site) anions are shown as yellow and orange spheres.

site. Moreover, the contribution to the X^O_M anion from the M^H cation is higher than that to the X^O_A anion from the A^P cation as the content of (Y + *REE*) is higher at the M^H site (Tables 6, 7). Calculation of bond-valence sums at the X^O_M and X^O_A anions (using cation-oxygen parameters) gave a lower sum for the X^O_A anion (Table 8). Therefore we assigned 2 F apfu to the X^O_A site. Chemical analysis gives 2.6 F apfu (Table 2), hence we subtract 2 apfu from the total F (Table 2) and assign the remaining 0.60 F apfu to the X^O_M site, which has the following composition: $(O_{1.40}F_{0.60})$.

The crystal structure

The crystal structure of rinkite-(Y) is a framework of TS (Titanium-Silicate) blocks. The TS block consists of HOH sheets (H – heteropolyhedral, O – octahedral) (Sokolova, 2006).

In the O sheet, there is one [6]-coordinated Ti-dominant M^O1 site, with $<M^O1–\varphi> = 1.987$ Å (Tables 6, 7). The M^O1 site ideally gives 1 Ti apfu. There are $^{[8]}M^O2$ and $^{[6]}M^O3$ sites, ideally occupied by 1 Na apfu and (NaCa) apfu, respectively (Tables 6, 7; Fig. 3*a*). The ideal composition of the O sheet, $M^O_4(X^O_M)_2(X^O_A)_2$, is $[Na(NaCa)Ti(OF)F_2]^{3+}$ or, in a shorter form, $[Na_2CaTiOF_3]^{3+}$ apfu (Tables 1,7).

In the H sheet, there are two [7]-coordinated Ca-dominant sites: M^H and A^P, which ideally give (Ca_3Y) apfu (Table 7). The two $^{[4]}Si$ sites are occupied solely by Si with <Si–O> = 1.623 Å. The M^H and A^P polyhedra and Si_2O_7 groups constitute the H sheet (Fig. 3*b*). The ideal composition of the two H sheets, $A^P_2M^H_2(Si_2O_7)_2$, is $[(Ca_3Y)(Si_2O_7)_2]^{3-}$ or, in a shorter form, $[Ca_3Y(Si_2O_7)_2]^{3-}$ apfu (Tables 1,7).

Linkage of H and O sheets via common vertices of M^H and A^P polyhedra and Si_2O_7 groups with $M^O1–3$ polyhedra results in a TS block (Fig. 3*c*). The TS block in rinkite-(Y) exhibits *linkage 1* of H and O sheets and stereochemistry typical for the rinkite group (Ti = 1 apfu) (Sokolova, 2006): two H sheets connect to the O sheet such that two Si_2O_7 groups link to the *trans* edges of an $^{[8]}Na$ polyhedron of the O sheet. In the crystal structure of rinkite-(Y), two adjacent TS blocks are related by the c_y glide plane.

For rinkite-(Y), we write the ideal structural formula of the form $A^P_2M^H_2M^O_4(Si_2O_7)_2(X^O_M)_2(X^O_A)_2$ as the sum of the ideal compositions of the O sheet and two H sheets: $[Na(NaCa)Ti(OF)F_2]^{3+} + [(Ca_3Y)(Si_2O_7)_2]^{3-} = (Ca_3Y)Na(NaCa)Ti(Si_2O_7)_2(OF)F_2$ with $Z = 2$. We write the ideal formula of rinkite as the sum of the ideal compositions of the O sheet and two H sheets in shorter forms: $[Ca_3Y(Si_2O_7)_2]^{3-} + [Na_2CaTiOF_3]^{3+} = Na_2Ca_4YTi(Si_2O_7)_2OF_3$.

Summary

Rinkite-(Y) differs from rinkite-(Ce) in the dominant rare-earth element, Y versus Ce, respectively. In accord with Bayliss and Levinson (1988), the mineral is named rinkite-(Y) as it is structurally identical to rinkite-(Ce). Table 9 lists comparative data for rinkite-(Y) and rinkite-(Ce).

Acknowledgements. We thank reviewers F. Cámara and P. Leverett and Associate Editor I. Graham for their useful comments which helped to improve the manuscript. We are grateful to A.R. Faiziev, P.V. Kvorov and R.U. Sobirova for their help in organisation and carrying-out the fieldwork. This work was supported by a Canada Research Chair in Crystallography and Mineralogy and by a Discovery grant from the Natural Sciences and Engineering Research Council of Canada to FCH, and by Innovation Grants from the Canada Foundation for Innovation to FCH.

Supplementary material. To view supplementary material for this article, please visit https://doi.org/10.1180/mgm.2018.122.

References

Anthony J.W., Bideaux R.A., Bladh K.W. and Nichols M.C. (1995) *Handbook of Mineralogy*. II. *Silica, Silicates*. Part 2. Mineral Data Publishing, Tucson, p. 689.

Bayliss P. and Levinson A.A. (1988) A system of nomenclature for rare-earth mineral species: Revision and extension. *American Mineralogist*, **73**, 422–423.

Belakovskiy D.I. (1991) Die seltenen Mineralien von Dara-i-Pioz im Hochgebirge Tadshikistans. *Lapis*, **16**, 42–48.

Bellezza M., Franzini M., Larsen A.O., Merlino S. and Perchiazzi N. (2004) Grenmarite, a new member of the götzenite-seidozerite-rosenbuschite group from the Langesundsfjord district, Norway: definition and crystal structure. *European Journal of Mineralogy*, **16**, 971–978.

Blumrich J. (1893) Die Phonolithe des Friedländer Bexirkes in Nordböhmen. *Tschermaks Mineralogische und Petrographische Mitteilungen*, **13**, 465–495.

Brögger W.C. (1887) Forelöbig meddelelse om mineralerne på de sydnorske augit- og nefelinsyeniters grovkornige gange. *Geologiska Föreningens i Stockholm Förhandlingar*, **109**, 247–274.

Brögger W.C. (1890) Die miniralien der syenitpegmatitgänge der südnorwegischen augit und nephelinsyenite. *Zeitschrift für Kristallographie und Mineralogie*, **16**, 74–94.

Brown I.D. (1981) The bond-valence method: an empirical approach to chemical structure and bonding. Pp. 1–30 in: *Structure and Bonding in Crystals II* (M. O'Keeffe and A. Navrotsky, editors). Academic Press, New York.

Cámara F., Sokolova E. and Hawthorne F.C. (2011) From structure topology to chemical composition. XII. Titanium silicates: the crystal chemistry of rinkite, $Na_2Ca_4\mathit{REE}Ti(Si_2O_7)_2OF_3$. *Mineralogical Magazine*, **75**, 2755–2774.

Cámara F., Sokolova E., Abdu Y.A., Hawthorne F.C., Charrier T., Dorcet V. and Carpentier J.-F. (2017) Fogoite-(Y), $Na_3Ca_2Y_2Ti(Si_2O_7)_2OF_3$, a Group-I TS-block mineral from the Lagoa do Fogo, the Fogo volcano, the São Miguel Island, the Azores: description and crystal structure. *Mineralogical Magazine*, **81**, 383–342.

Chakrabarty A., Mitchell R.H., Ren M., Sen A.K. and Pluseth K.L. (2013) Rinkite, cerianite-(Ce) and hingganite-(Ce) in syenite gneisses from the Sushina Hill Complex, India: occurrence, compositional data and petrogenetic significance. *Mineralogical Magazine*, **77**, 3137–3153.

Christiansen C.C., Johnsen O. and Makovicky E. (2003*a*) Crystal chemistry of the rosenbuschite group. *The Canadian Mineralogist*, **41**, 1203–1224.

Christiansen C.C., Gault R.A., Grice J.D. and Johnsen O. (2003*b*) Kochite, a new member of the rosenbuschite group from the Werner Bjerge alkaline complex, East Greenland. *European Journal of Mineralogy*, **15**, 551–554.

Dusmatov V.D. (1968) On mineralogy of one alkaline massif. Pp. 134–135 in: *Alkaline Rocks of Kirgizia and Kazakhstan*, Ilym, Frunze [in Russian].

Dusmatov V.D. (1971) *Mineralogy of the Darai-Pioz Alkaline Massif (Southern Tien-Shan)*. PhD dissertation, Institute of Mineralogy, Geochemistry and Crystal Chemistry of Rare Elements, Moscow, 171 p. [in Russian].

Faiziev A.R., Gafurov F.G. and Sharipov B.N. (2010) Carbonatites of the Darai-Pioz alkaline massif, Central Tadjikistan, and their compositional features. *Geochemistry International*, **48**, 1084–1096.

Galli E. and Alberti A. (1971) The crystal structure of rinkite. *Acta Crystallographica*, **B27**, 1277–1284.

Kheirov M.B., Mamedov Kh.S. and Belov N.V. (1963) Crystal structure of rinkite, $Na(Ca,Ce)_2(Ti,Ce)O(Si_2O_7)F$. *Doklady Akademii Nauk SSSR*, **150**, 162–164.

Lorenzen J. (1884) Untersuchung einiger Mineralien aus Kangerdluarsuk in Grönland. *Zeitschrift für Kristallographie*, **9**, 243–254.

Lyalina L., Zolotarev Jr. A., Selivanova E., Savchenko E., Zozulya D., Krivovichev S. and Mikhailova Yu. (2015) Structural characterization and composition of Y-rich hainite from Sakharjok nepheline syenite pegmatite (Kola Peninsula, Russia). *Mineralogy and Petrology*, **109**, 443–451.

Lyalina L.M., Zolotarev Jr. A.A., Selivanova E.A., Savchenko Ye.E., Krivovichev S.V., Mikhailova Yu.A., Kadyrova G.I. and Zozulya D.R. (2016) Batievaite-(Y), $Y_2Ca_2Ti[Si_2O_7]_2(OH)_2(H_2O)_4$, a new mineral from nepheline syenite pegmatite in the Sakharjok massif, Kola Peninsula, Russia. *Mineralogy and Petrology*, **110**, 895–904.

Mandarino J.A. (1981) The Gladstone-Dale relationship. IV. The compatibility index and its application. *The Canadian Mineralogist*, **19**, 441–450.

Mineev D.A. (1969) *Lantanoides in minerals*. Nedra, Moscow, 184 pp. [in Russian].

Moskvin A.V. (1937) Geography and Geology of East Karategin. Pp. 682–739 in: *Tajik-Pamir Expedition of 1935*. Academy of Sciences of USSR, Moscow–Leningrad [in Russian].

Pautov L.A., Agakhanov A.A., Karpenko V.Y., Uvarova Y.A., Sokolova E. and Hawthorne F.C. (2017) Rinkite-(Y), IMA 2017-043. CNMNC Newsletter No. 39, October 2017, page 1280; *Mineralogical Magazine*, **81**, 1279–1286.

Petersen O.V., Rønsbo J.G. and Leonardsen E.S. (1989) Nacareniobsite-(Ce), a new mineral species from the Ilímaussaq alkaline complex, South Greenland, and its relation to mosandrite and the rinkite series. *Neues Jahrbuch für Mineralogie – Monatshefte*, No. 2, 84–96.

Pouchou J.L. and Pichoir F. (1985) "PAP" (φ(ρz)) procedure for improved quantitative microanalysis. Pp. 104–106 in: *Microbeam Analysis* (J.T. Armstrong, editor). San Francisco Press, San Francisco, California, USA.

Rastsvetaeva R.K, Borutskii B.E. and Shlyukova Z.V. (1991) Crystal structure of Hibbing (Khibinian) rinkite. *Soviet Physics Crystallography*, **36**, 349–351.

Reguir E.P., Chakhmouradian A.R. and Evdokimov M.D. (1999) The mineralogy of a unique baratovite- and miserite-bearing quartz – albite – aegirine rock from the Dara-i-Pioz complex, northern Tajikistan. *The Canadian Mineralogist*, **37**, 1369–1384.

Rønsbo J.G., Sørensen H., Roda-Robles E., Fontan F. and Monchoux P. (2014) Rinkite–nacareniobsite-(Ce) solid solution series and hainite from the Ilímaussaq alkaline complex: occurrence and compositional variation. *Bulletin of the Geological Society of Denmark*, **62**, 1–15.

Sahama Th.G. and Hytönen M.A. (1957) Gotzenite and combeite, two new silicates from the Belgian Congo. *Mineralogical Magazine*, **31**, 503–510.

Semenov E.I. (1963) *Mineralogy of Rare Earths*. Pp. 186–190. Academy of Sciences of USSR, Moscow [in Russian].

Semenov E.I. and Dusmatov V.D. (1975) On mineralogy of the Darai-Pioz alkaline massif (Central Tajikistan). *Doklady Akademii nauk Tadzhikskoi SSR*, **XVIII**, 39–41 [in Russian].

Semenov E.I., Kazakova M.E. and Simonov V.I. (1958) A new zircon mineral seidoserite and other minerals of the wohlerite group in alkaline pegmatites. *Zapiski Vsesoyuznogo Mineralogicheskogo Obshchestva*, **87**, 590–597 [in Russian].

Shannon R.D. (1976) Revised effective ionic radii and systematic studies of interatomic distances in halides and chalcogenides. *Acta Crystallographica*, **A32**, 751–767.

Sheldrick G.M. (2008) A short history of SHELX. *Acta Crystallographica*, **A64**, 112–122.

Sheldrick G.M. (2015) Crystal structure refinement with SHELXL. *Acta Crystallographica*, **C71**, 3–8.

Simonov V.I. and Belov N.V. (1968) Characteristics of the crystal structure of rinkite. *Soviet Physics Crystallography*, **12**, 740–744.

Slepnev Yu.S. (1957) On the minerals of the rinkite group. *Izvestiya Akademii Nauk SSSR, Seriya Geologicheskaya*, **N3**, 63–75 [in Russian].

Sokolova E. (2006) From structure topology to chemical composition. I. Structural hierarchy and stereochemistry in titanium disilicate minerals. *The Canadian Mineralogist*, **44**, 1273–1330.

Sokolova E. and Cámara F. (2008) From structure topology to chemical composition. VIII. Titanium silicates: the crystal structure and crystal chemistry of mosandrite from type locality of Låven (Skådön), Langesundsfjorden, Larvik, Vestfold, Norway. *Mineralogical Magazine*, **72**, 887–897.

Sokolova E. and Cámara F. (2013) From structure topology to chemical composition. XVI. New developments in the crystal chemistry and prediction of new structure topologies for titanium disilicate minerals with the TS block. *The Canadian Mineralogist*, **51**, 861–891.

Sokolova E. and Cámara F. (2017) The seidozerite supergroup of TS-block minerals: nomenclature and classification, with change of the following names: rinkite to rinkite-(Ce), mosandrite to mosandrite-(Ce), hainite to hainite-(Y) and innelite-1*T* to innelite-1*A*. *Mineralogical Magazine*, **81**, 1457–1484.

Sokolova E. and Hawthorne F.C. (2008) From structure topology to chemical composition. V. Titanium silicates: crystal chemistry of nacareniobsite-(Ce). *The Canadian Mineralogist*, **46**, 1333–1342.

Sokolova E. and Hawthorne F.C. (2013) From structure topology to chemical composition. XIV. Titanium silicates: refinement of the crystal structure and revision of the chemical formula of mosandrite, $(Ca_3\mathit{REE})[(H_2O)_2Ca_{0.5}\square_{0.5}]Ti(Si_2O_7)_2(OH)_2(H_2O)_2$, a Group-I mineral from the Saga mine, Morje, Porsgrunn, Norway. *Mineralogical Magazine*, **77**, 2753–2771.

Tê-yü L., Simonov V.I. and Belov N.I. (1965) Crystal structure of rinkite $Na(Na,Ca)_2(Ca,Ce)_4\ (Ti,Nb)[Si_2O_7]_2(O,F)_2F_2$. *Soviet Physics Doklady*, **10**, 496–498.

Wilson A.J.C. (editor) (1992) *International Tables for Crystallography. Volume C: Mathematical, Physical and Chemical tables*. Kluwer Academic Publishers, Dordrecht, The Netherlands.